

1 **Anthracene-based ferrocenylselenoethers: syntheses, crystal structures, Cu(I) complexes and sensing property**

2 Yu-Qing Liu<sup>a</sup>, Wei Ji<sup>a,b</sup>, Hai-Yan Zhou<sup>a</sup>, Yu Li<sup>a</sup>, Su Jing<sup>\*,a</sup>, Dun-Ru Zhu<sup>\*,b</sup>, Jian Zhang<sup>c</sup>

3

4 <sup>a</sup>College of Sciences, Nanjing Tech University, Nanjing 211816, P.R. China. E-mail: [sjing@njtech.edu.cn](mailto:sjing@njtech.edu.cn).

5 <sup>b</sup>College of Chemistry and Chemical Engineering, Nanjing Tech University, Nanjing 210009, P.R. China. E-mail: [zhudr@njtech.edu.cn](mailto:zhudr@njtech.edu.cn).

6 <sup>c</sup>Laboratory of Translational Medicine, Jiangsu Province Academy of Traditional Chinese Medicine, Nanjing 210028, P.R. China.

7

8 **Table of contents**

9

10 **Fig. S1:** <sup>1</sup>H NMR spectrum of **L3**, CDCl<sub>3</sub>, 298 K.

11 **Fig. S2:** <sup>1</sup>H NMR spectrum of **L4**, CDCl<sub>3</sub>, 298 K.

12 **Fig. S3:** <sup>1</sup>H NMR spectrum of **L5**, CDCl<sub>3</sub>, 298 K.

13 **Fig. S4:** MALDI-TOF Spectrum of **L3**

14 **Fig. S5:** MALDI-TOF Spectrum of **L4**

15 **Fig. S6:** ESI-MS spectrum of **L5**

16 **Fig. S7:** Fluorescence spectra change of **L3** ( $1 \times 10^{-4}$  M) in a CH<sub>2</sub>Cl<sub>2</sub> solution upon addition of various metal ions.

17 **Fig. S8:** Fluorescence spectra change of **L4** ( $1 \times 10^{-4}$  M) in a CH<sub>2</sub>Cl<sub>2</sub> solution upon addition of various metal ions.

18 **Fig. S9:** UV/vis spectra changes of receptor **L3** ( $1 \times 10^{-4}$  M) in a CH<sub>2</sub>Cl<sub>2</sub> solution upon the addition of various metal ions.

19 **Fig. S10:** UV/vis spectra changes of receptor **L4** ( $1 \times 10^{-4}$  M) in a CH<sub>2</sub>Cl<sub>2</sub> solution upon the addition of various metal ions.

20 **Fig. S11:** UV/vis spectra changes of receptor **L5** ( $1 \times 10^{-4}$  M) in a CH<sub>2</sub>Cl<sub>2</sub> solution upon the addition of various metal ions.

21 **Fig.S12:** Absorbance of **L5** at different concentrations of Zn<sup>2+</sup> added, normalized between the minimum absorbance and the maximum  
22 absorbance intensity. The detection limit was determined to be  $6.62 \times 10^{-6}$  M.

23 **Fig.S13:** Benesi-Hilderbrand plot of **L5** with Zn(ClO<sub>4</sub>)<sub>2</sub>.

24 **Fig.S14:** Absorbance of **L5** at different concentrations of  $\text{Cu}^{2+}$  added, normalized between the minimum absorbance and the maximum  
25 absorbance intensity. The detection limit was determined to be  $5.26 \times 10^{-5} \text{M}$ .

26 **Fig.S15:** Benesi-Hilderbrand plot of **L5** with  $\text{Cu}(\text{ClO}_4)_2$ .

27 **Fig.S16:** Cyclic voltammogram of **L3** (black line) in  $\text{CH}_3\text{CN}/\text{CH}_2\text{Cl}_2$  (1:1, v/v) solution upon addition of excess  $\text{Cu}(\text{ClO}_4)_2$  (red line) and  
28  $\text{Hg}(\text{ClO}_4)_2$  (green line).

29 **Fig.S17:** Cyclic voltammogram of **L4** (black line) in  $\text{CH}_3\text{CN}/\text{CH}_2\text{Cl}_2$  (1:1, v/v) solution upon addition of excess  $\text{Cu}(\text{ClO}_4)_2$  (red line) and  
30  $\text{Hg}(\text{ClO}_4)_2$  (green line).

31 **Fig.S18:** Cyclic voltammogram of **L5** (black line) in  $\text{CH}_3\text{CN}/\text{CH}_2\text{Cl}_2$  (1:1, v/v) solution upon addition of excess  $\text{Cu}(\text{ClO}_4)_2$  (red line),  $\text{Zn}(\text{ClO}_4)_2$   
32 (blue line) and  $\text{Hg}(\text{ClO}_4)_2$  (green line).

33 **Fig.S19:** IR spectrum of **L5**

34 **Fig.S20:** IR spectrum of **L5** with excess  $\text{Cu}(\text{ClO}_4)_2$

35 **Fig.S21:** IR spectrum of **L5** with excess  $\text{Zn}(\text{ClO}_4)_2$

36 **Fig.S22:** IR spectrum of **L5** with excess  $\text{Hg}(\text{ClO}_4)_2$

37 **Table S1:** Selected Bond Lengths ( $\text{\AA}$ ) and Bond Angles ( $^\circ$ ) for **L3-L5**

38 **Table S2.** Selected Bond Lengths ( $\text{\AA}$ ) and Bond Angles ( $^\circ$ ) for **1-4**

39

40

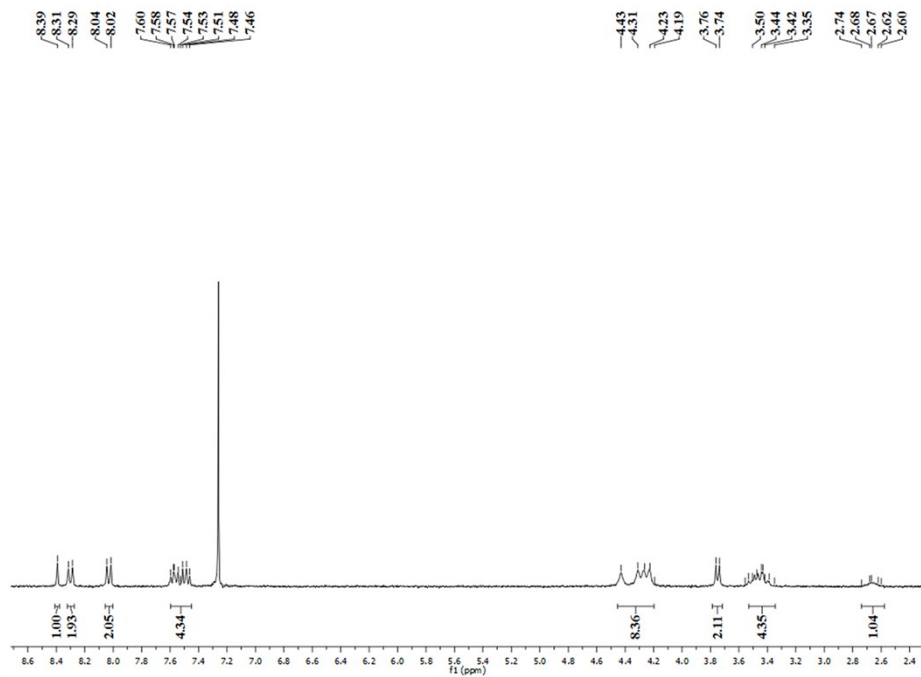
41

42

44 **Fig. S1:**  $^1\text{H}$  NMR spectrum of L3,  $\text{CDCl}_3$ , 298 K.

45

46

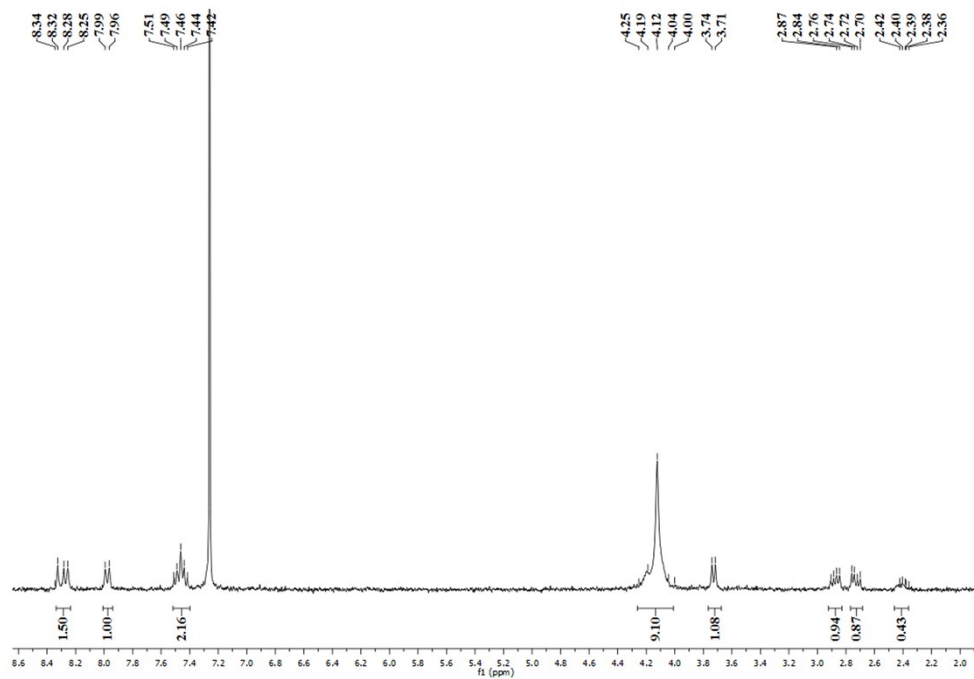


47

48

50 **Fig. S2:**  $^1\text{H}$  NMR spectrum of **L4**,  $\text{CDCl}_3$ , 298 K.

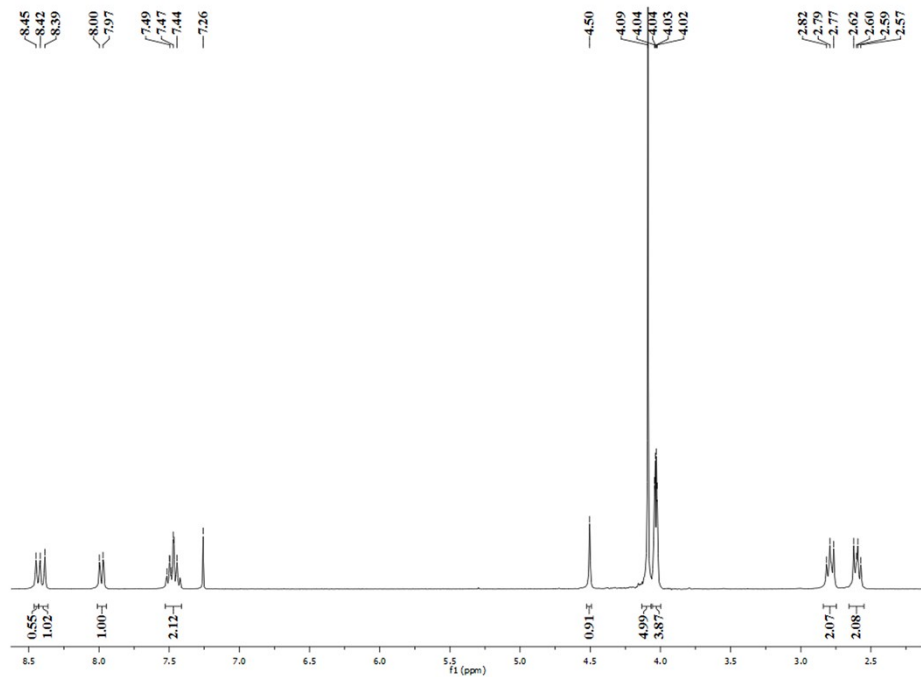
51



52

54 **Fig. S3:**  $^1\text{H}$  NMR spectrum of **L5**,  $\text{CDCl}_3$ , 298 K.

55

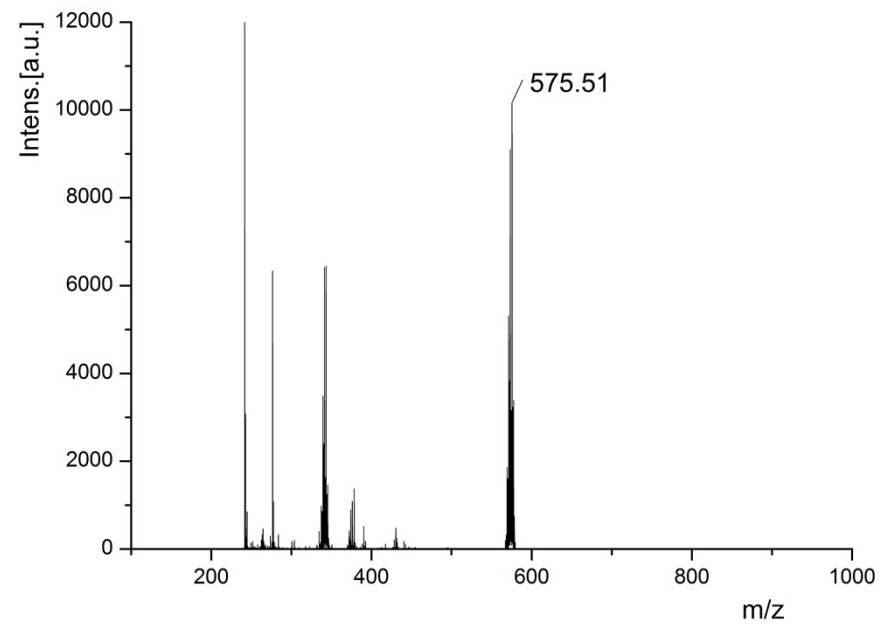


56

57

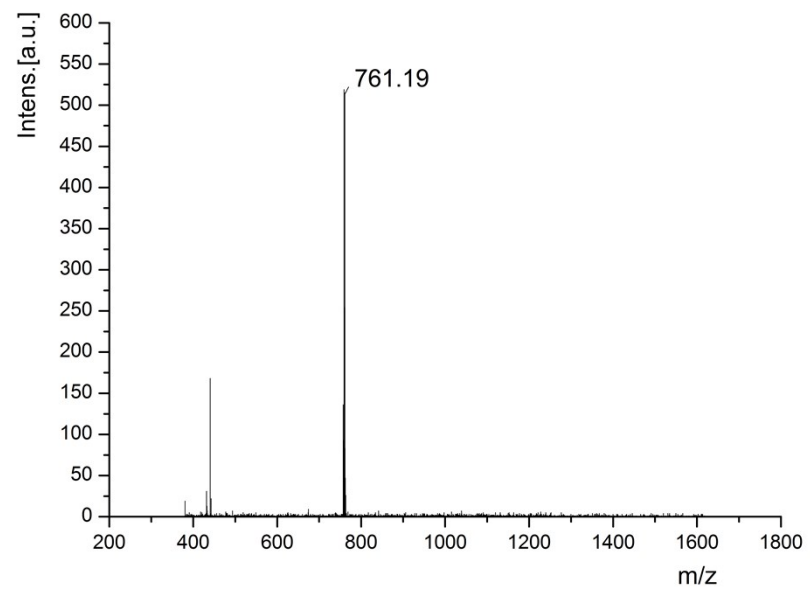
58

60 **Fig. S4: MALDI-TOF Spectrum of L3**



61  
62  
63  
64  
65  
66  
67  
68  
69

71 **Fig. S5: MALDI-TOF Spectrum of L4**



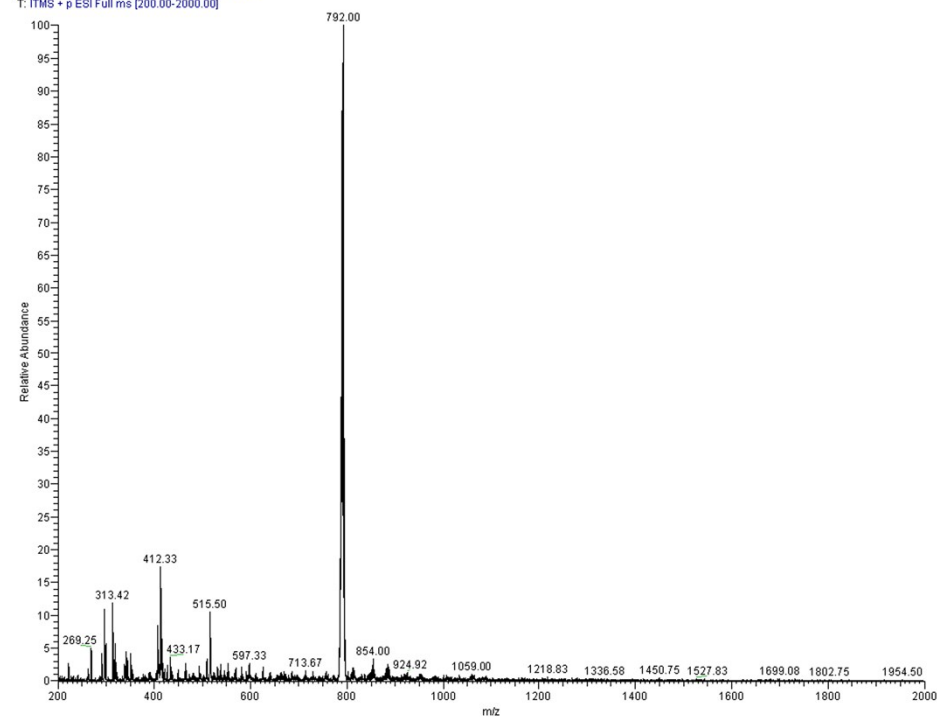
72  
73  
74

76 **Fig. S6: ESI-MS spectrum of L5**

77

D:\test\2013-1\Ngd\Jel\LYF1 3/29/2013 8:46:11 AM

LYF1 #9-33 RT: 0.04-0.16 AV: 25 NL: 1.20E3  
T: ITMS + p ESI Full ms [200.00-2000.00]



78

79

80

81

82

83

84

85

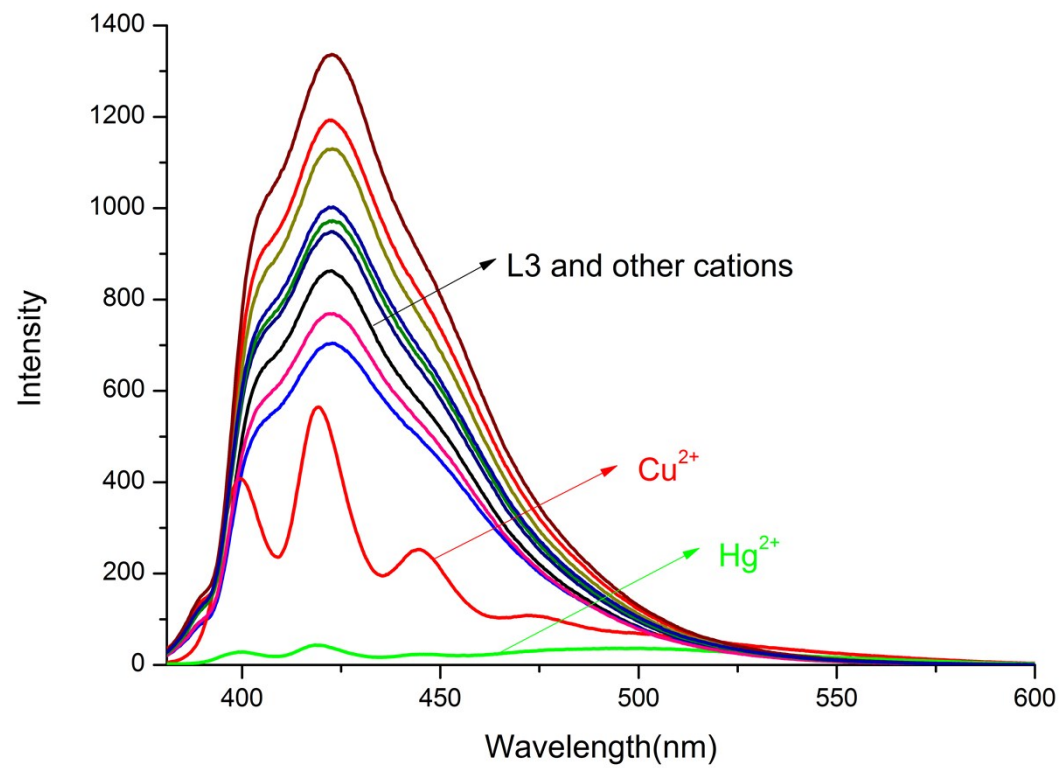
86



87

88 **Fig. S7:** Fluorescence spectra change of **L3** ( $1 \times 10^{-4}$  M) in a  $\text{CH}_2\text{Cl}_2$  solution upon addition of various metal ions.

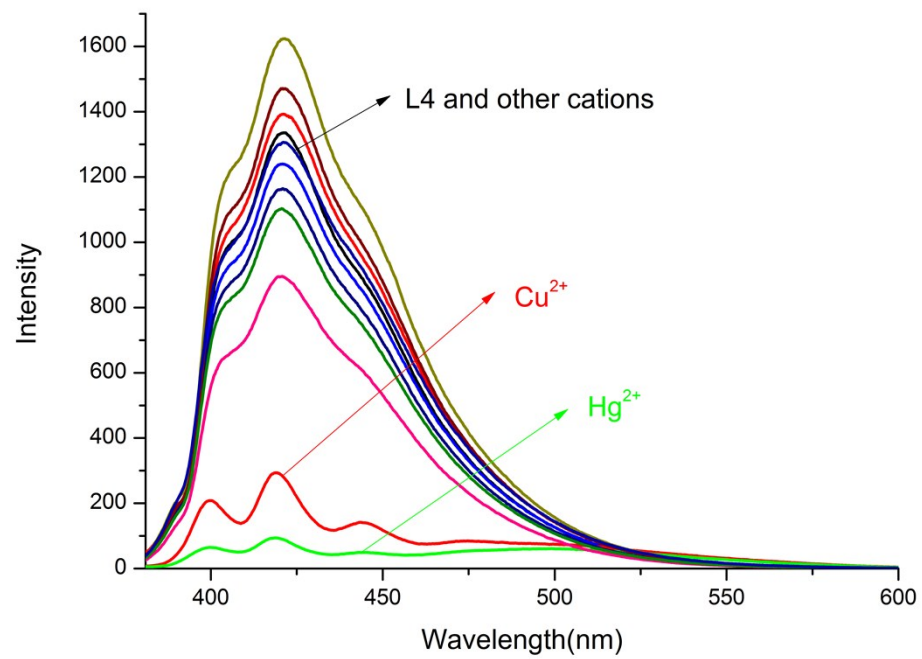
89



90

91

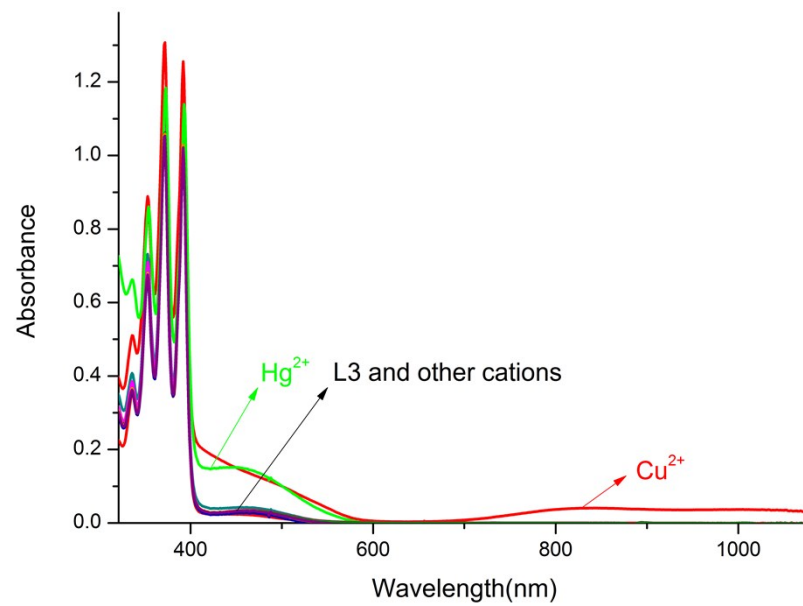
93 **Fig. S8:** Fluorescence spectra change of **L4** ( $1 \times 10^{-4}$  M) in a  $\text{CH}_2\text{Cl}_2$  solution upon addition of various metal ions  
94  
95



97 **Fig. S9:** UV/vis spectra changes of receptor **L3** ( $1 \times 10^{-4}$  M) in a  $\text{CH}_2\text{Cl}_2$  solution upon the addition of various metal ions.

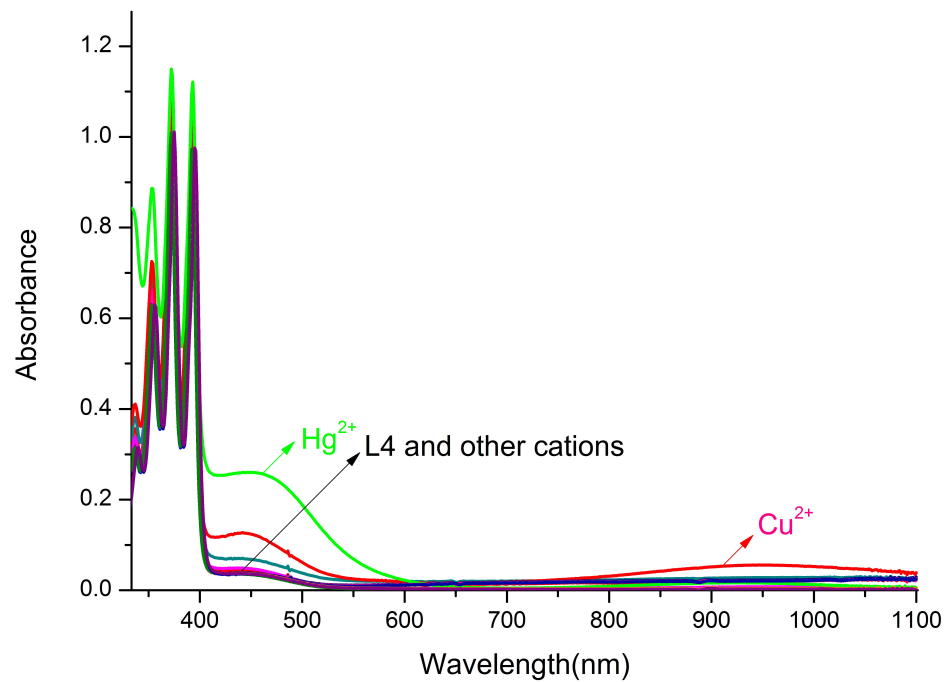
98

99



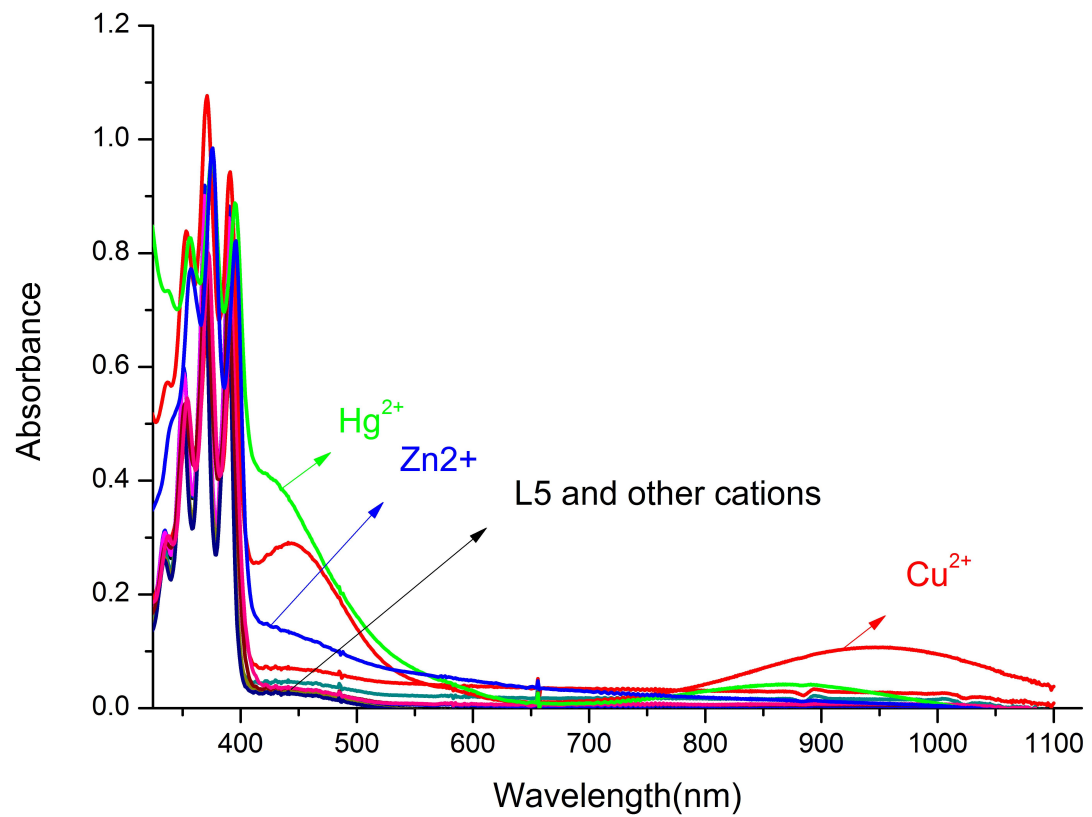
100

102 **Fig. S10:** UV/vis spectra changes of receptor **L4** ( $1 \times 10^{-4}$  M) in a  $\text{CH}_2\text{Cl}_2$  solution upon the addition of various metal ions.



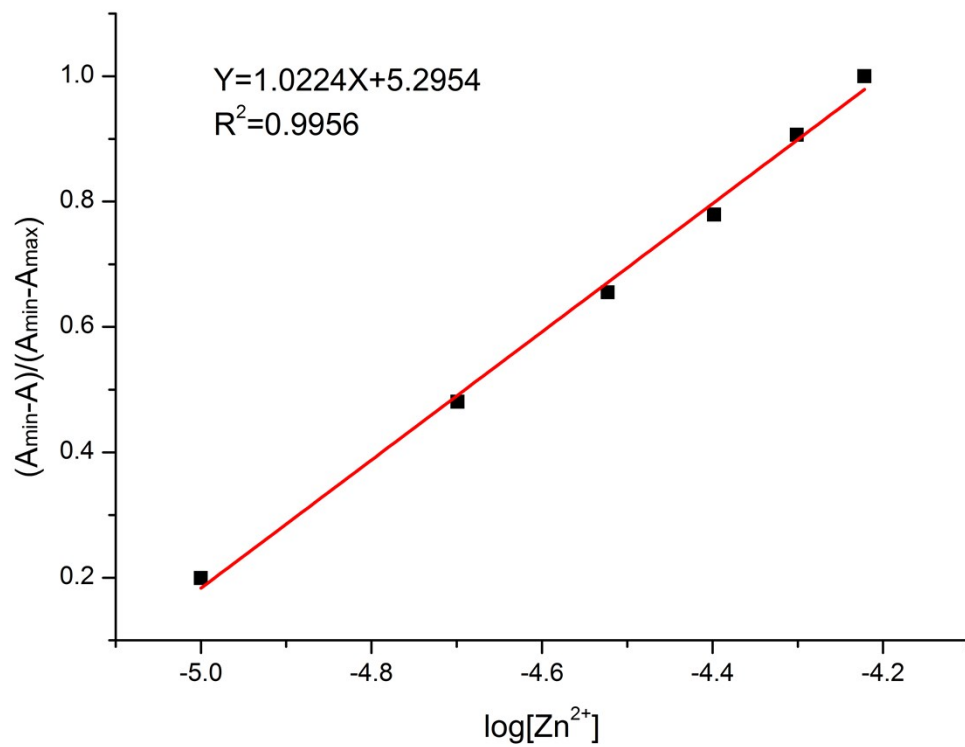
103  
104  
105  
106  
107  
108

110 **Fig. S11:** UV/vis spectra changes of receptor **L5** ( $1 \times 10^{-4}$  M) in a  $\text{CH}_2\text{Cl}_2$  solution upon the addition of various metal ions.  
111



112  
113  
114

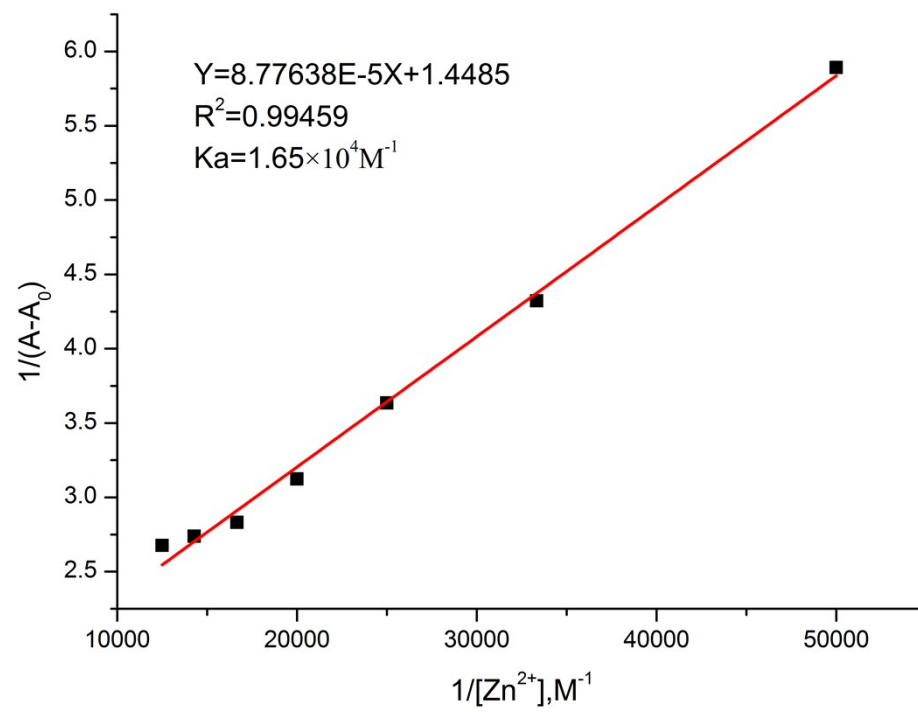
116 **Fig.S12:** Absorbance of **L5** at different concentrations of  $\text{Zn}^{2+}$  added, normalized between the minimum absorbance and the maximum  
117 absorbance intensity. The detection limit was determined to be  $6.62 \times 10^{-6}$  M.  
118



122 **Fig.S13:** Benesi-Hilderbrand plot of **L5** with  $\text{Zn}(\text{ClO}_4)_2$ .

123

124

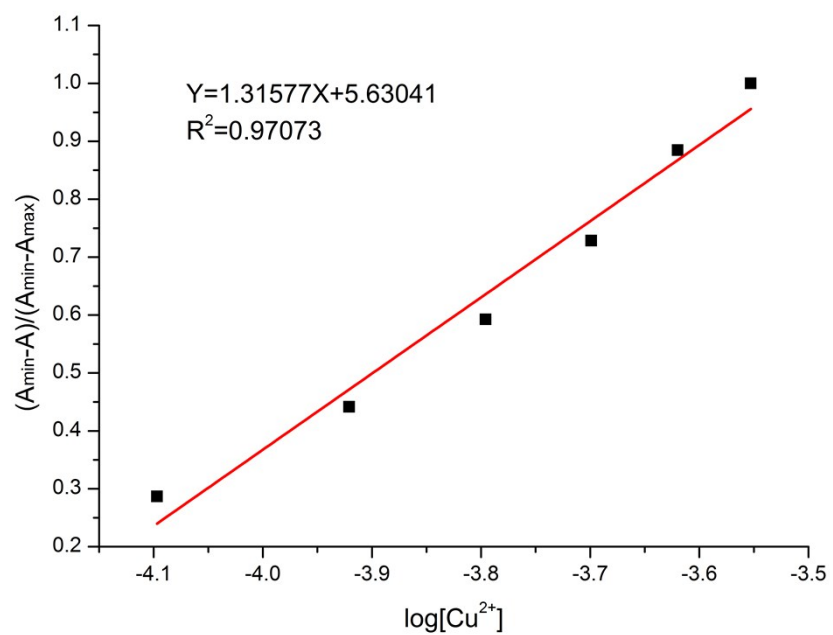


125

127 **Fig.S14:** Absorbance of **L5** at different concentrations of  $\text{Cu}^{2+}$  added, normalized between the minimum absorbance and the maximum  
128 absorbance intensity. The detection limit was determined to be  $5.26 \times 10^{-5} \text{M}$ .

129

130



131

132

133

134

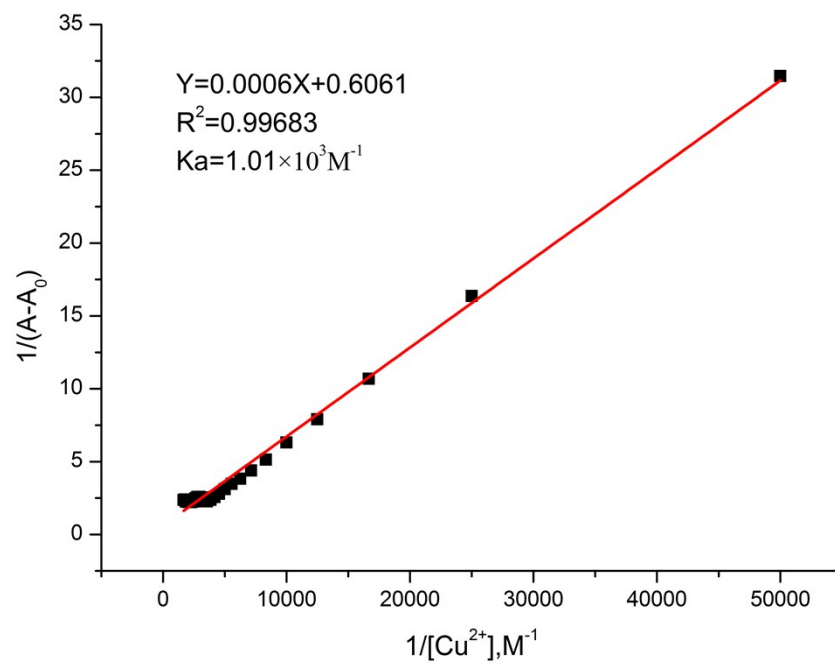
135



137 **Fig.S15:** Benesi-Hilderbrand plot of **L5** with  $\text{Cu}(\text{ClO}_4)_2$ .

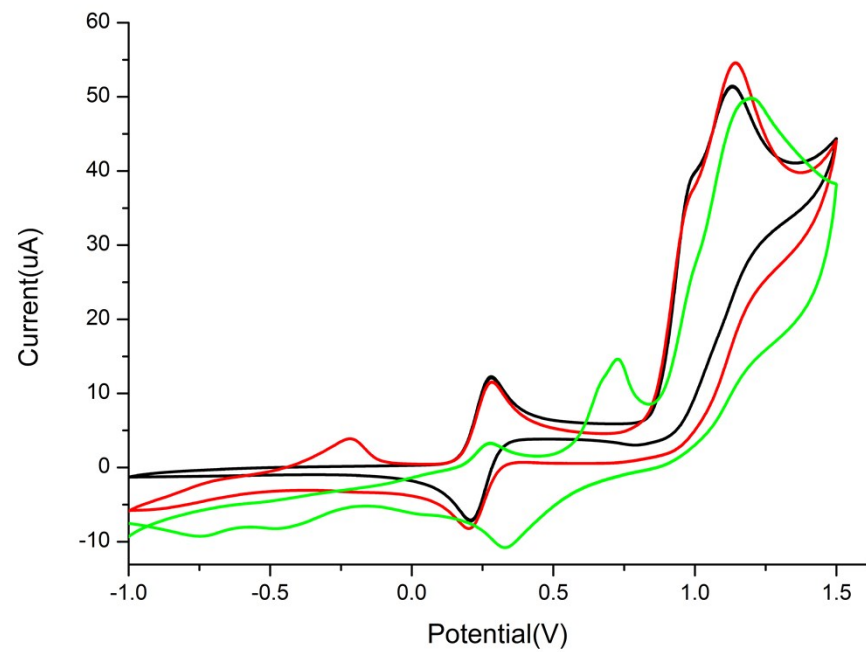
138

139



140

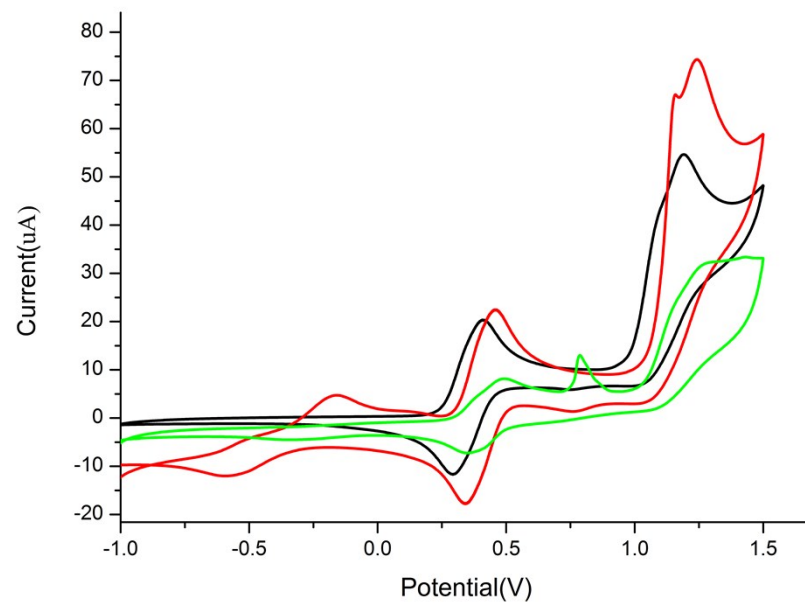
142 **Fig. S16:** Cyclic voltammogram of **L3** (black line) in CH<sub>3</sub>CN/CH<sub>2</sub>Cl<sub>2</sub> (1:1, v/v) solution upon addition of excess Cu(ClO<sub>4</sub>)<sub>2</sub> (red line) and  
143 Hg(ClO<sub>4</sub>)<sub>2</sub> (green line).  
144



145  
146  
147

149 **Fig. S17:** Cyclic voltammogram of **L4** (black line) in CH<sub>3</sub>CN/CH<sub>2</sub>Cl<sub>2</sub> (1:1, v/v) solution upon addition of excess Cu(ClO<sub>4</sub>)<sub>2</sub> (red line) and  
150 Hg(ClO<sub>4</sub>)<sub>2</sub> (green line).

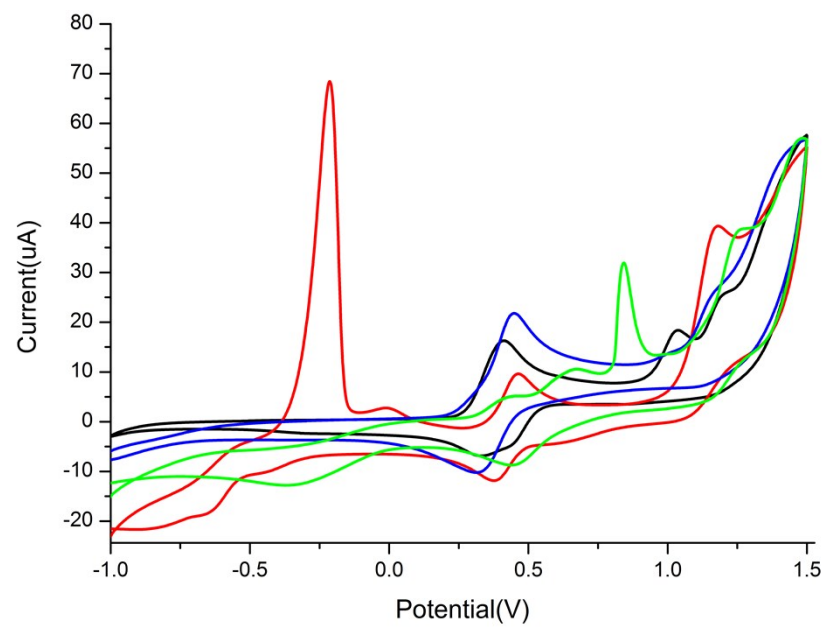
151



152  
153  
154  
155  
156  
157  
158

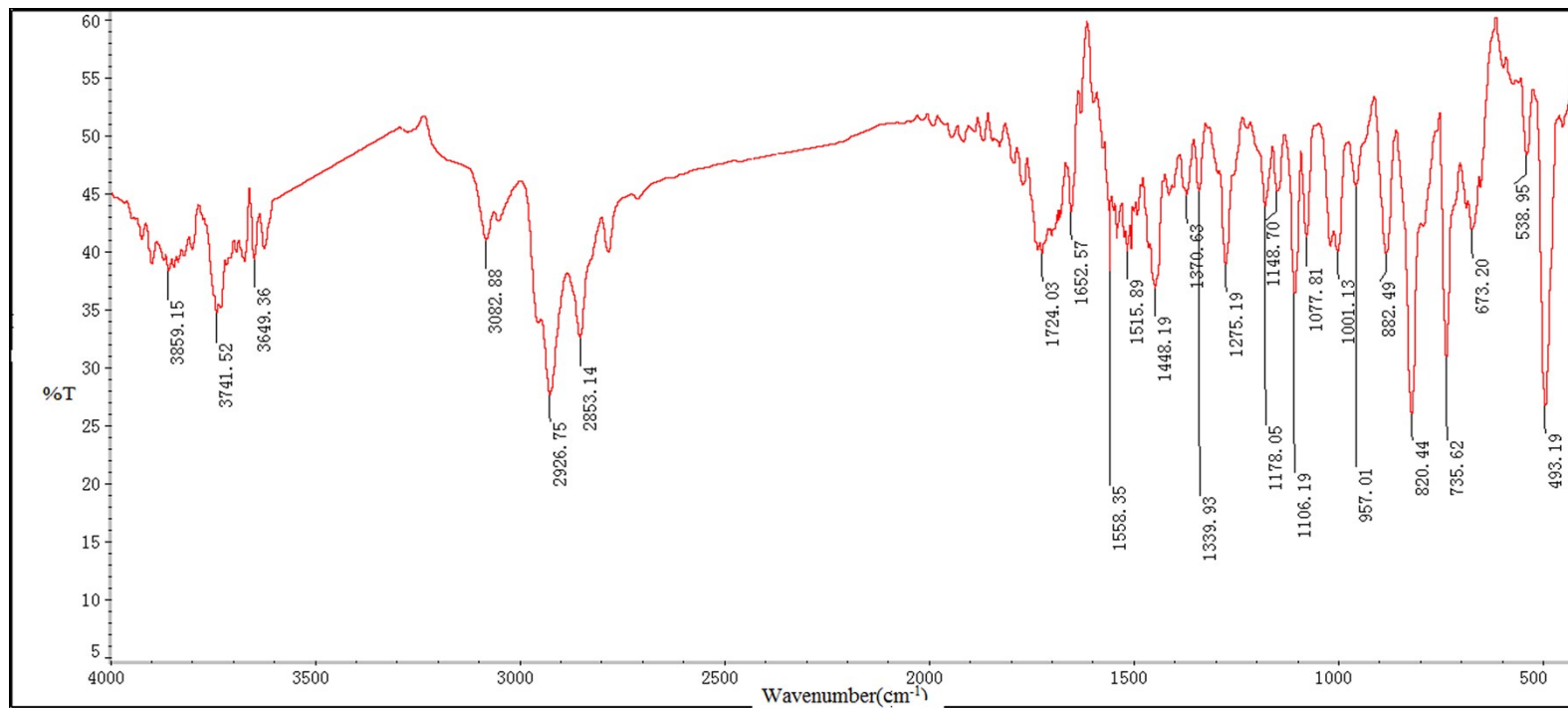
160 **Fig.S18:** Cyclic voltammogram of **L5** (black line) in  $\text{CH}_3\text{CN}/\text{CH}_2\text{Cl}_2$  (1:1, v/v) solution upon addition of excess  $\text{Cu}(\text{ClO}_4)_2$  (red line),  $\text{Zn}(\text{ClO}_4)_2$   
161 (blue line) and  $\text{Hg}(\text{ClO}_4)_2$  (green line).

162

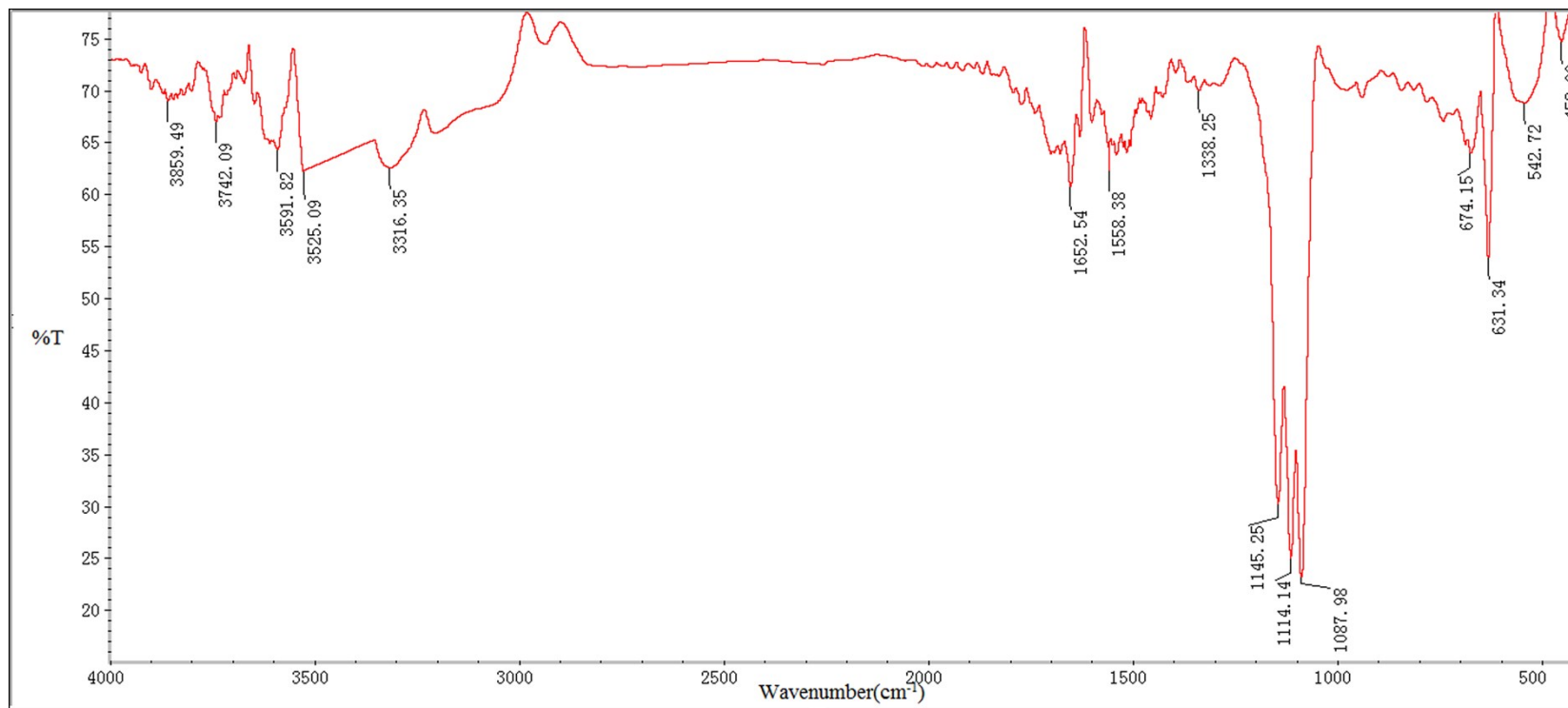


163

165 **Fig.S19:** IR spectrum of L5



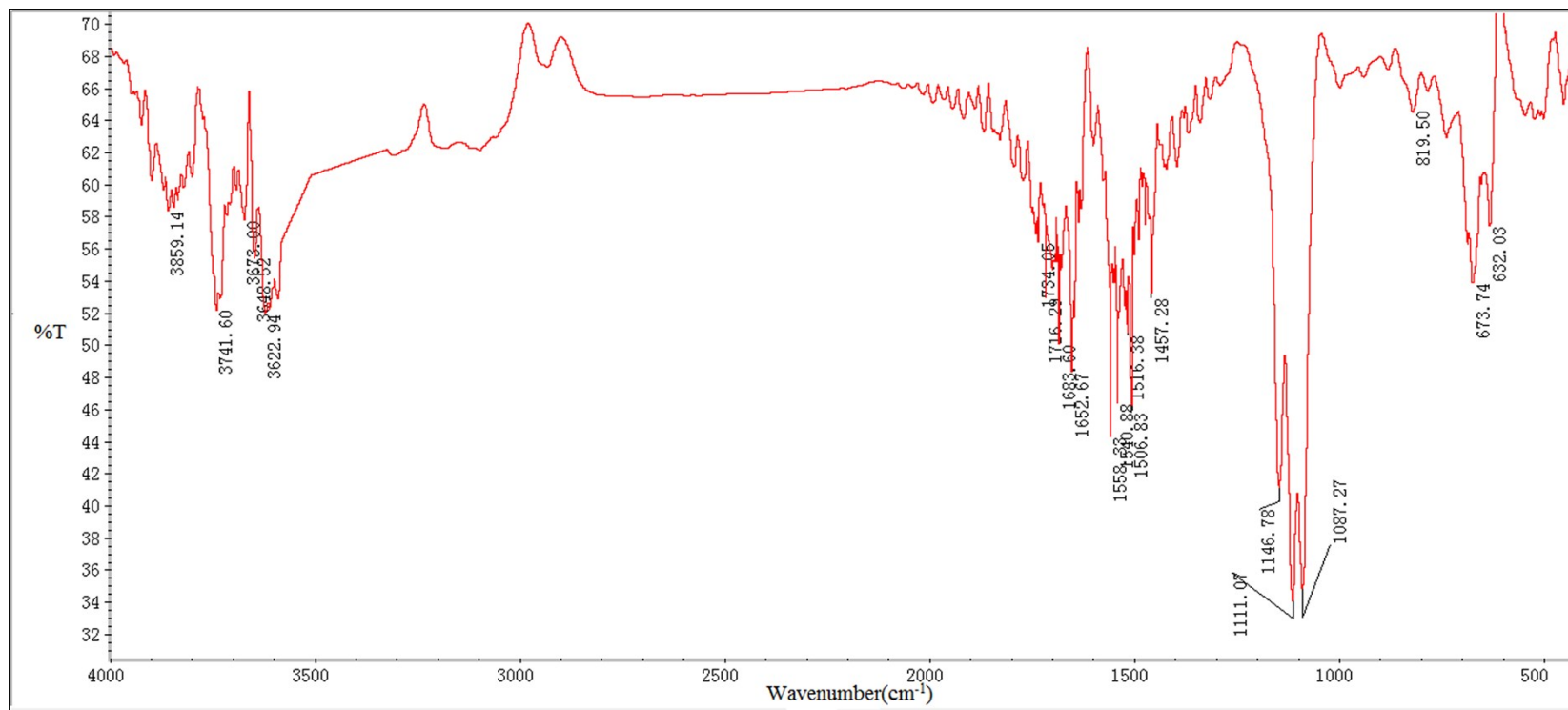
168 **Fig.S20:** IR spectrum of **L5** with excess  $\text{Cu}(\text{ClO}_4)_2$



169

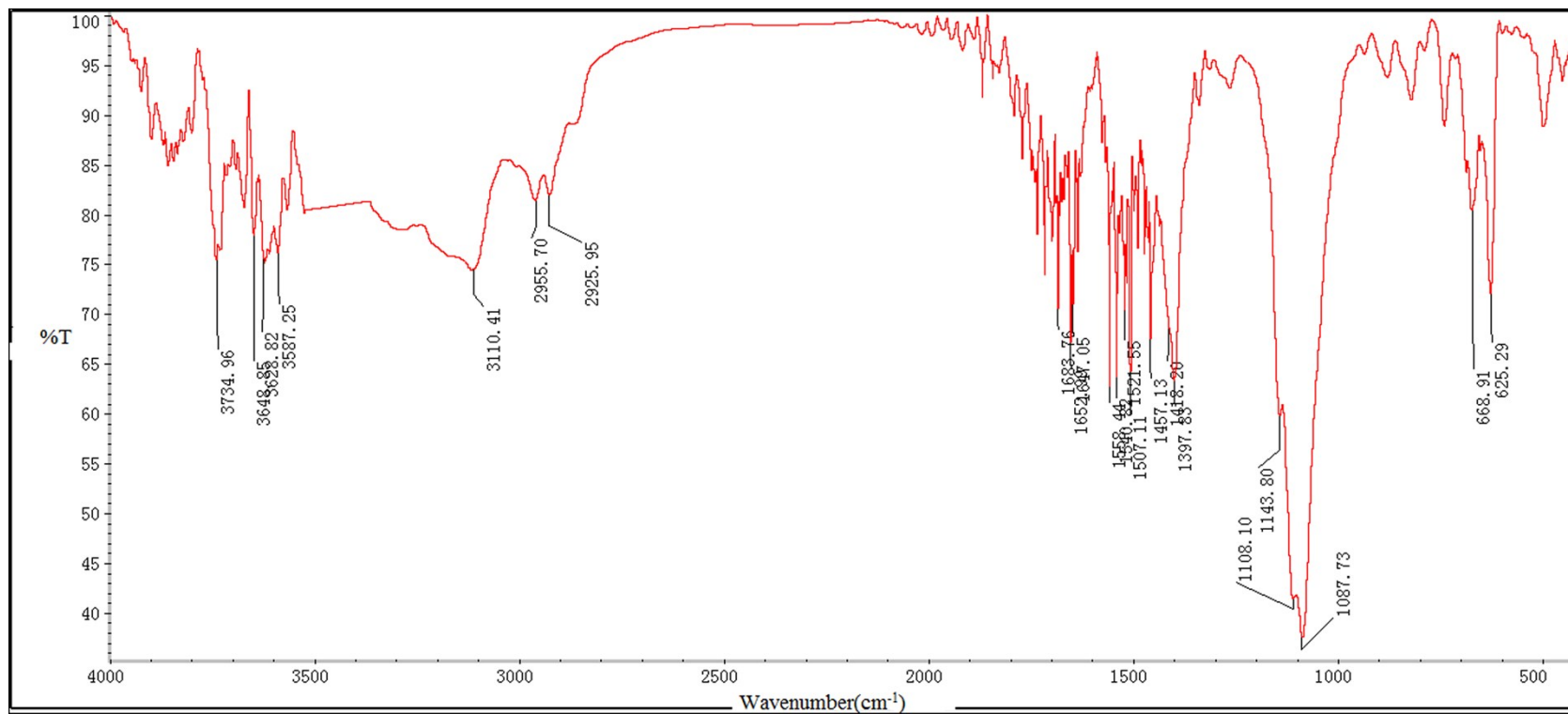
171 **Fig.S21:** IR spectrum of **L5** with excess  $\text{Zn}(\text{ClO}_4)_2$

172



173

175 **Fig.S22:** IR spectrum of **L5** with excess  $\text{Hg}(\text{ClO}_4)_2$



176



178 **Table S1:** Selected Bond Lengths (Å) and Bond Angles (°) for **L3-L5**

179

<b>L3</b>		<b>L4</b>		<b>L5</b>	
Se1-C1	1.898(5)	Se1-C11	1.902(4)	Se1-C1	1.907(4)
Se1-C11	1.966(6)	Se1-C23	1.958(4)	Se1-C21	1.968(4)
Se2-C6	1.912(5)	Se2-C1	1.902(3)	Se2-C11	1.913(4)
Se2-C13	1.954(5)	Se2-C21	1.974(4)	Se2-C24	1.969(9)
				N1-C25	1.463(4)
				N1-C22	1.470(4)
				N1-C23	1.478(4)
C1-Se1-C11	97.3(2)	C11-Se1-C23	100.53(2)	C1-Se1-C21	98.85(2)
C6-Se2-C13	104.4(2)	C1-Se2-C21	97.64(2)	C11-Se2-C24	94.45(2)
				C25-N1-C22	110.8(3)
				C25-N1-C23	111.4(3)
				C22-N1-C23	113.8(3)

180

181 **Table S2:** Selected Bond Lengths (Å) and Bond Angles (°) for **1-4**

182

	<b>1</b>	<b>2</b>	<b>3</b>	<b>4</b>			
Se1-C1	1.904(4)	Se1-C1	1.896(4)	Se1-C1	1.906(1)	Se1-C18	1.888(7)
Se1-C11	1.967(4)	Se1-C11	1.984(5)	Se1-C11	1.962(1)	Se1-C17	1.975(6)
Se2-C6	1.915(4)	Se2-C6	1.902(5)	Se2-C6	1.914(9)	Se2-C30	1.878(7)
Se2-C27	1.962(4)	Se2-C27	1.971(5)	Se2-C13	1.967(1)	Se2-C29	1.964(7)
Cu-Cu#1	2.793(1)	Cu1-Cu1#1	2.782(1)	Cu1-Cu2	2.612(2)	Se1-Cu1	2.436(1)
Se1-Cu	2.433(7)	Se1-Cu1	2.454(8)	Se1-Cu1	2.430(2)	Se2-Cu2#1	2.415(1)
Se2-Cu	2.436(7)	Se2-Cu1	2.451(8)	Se2-Cu1	2.444(2)	Se3-Cu3	2.433(1)
Br-Cu	2.452(7)	I1-Cu1	2.602(7)	Se3-Cu2	2.430(2)	Se4-Cu4#2	2.428(1)
Br-Cu#1	2.492(7)	I1-Cu1#1	2.627(8)	Se4-Cu2	2.433(2)	Cu2-Se2#1	2.415(1)
Cu-Br#1	2.492(7)	Cu1-I1#1	2.627(8)	I2-Cu1	2.566(2)	Cu4-Se4#2	2.428(1)
				I2-Cu2	2.663(2)	Cu1-Cu3	2.768(2)
				I1-Cu2	2.557(2)	Cu1-Cu4	2.886(2)
				I1-Cu1	2.638(2)	Cu1-Cu2	2.811(2)
Se1-Cu-Se2	114.55(2)	Se2-Cu1-Se1	112.40(3)	Se1-Cu1-Se2	99.72(6)	Cu2-Cu3	2.788(2)
Se1-Cu-Br	109.77(3)	Se1-Cu1-I1	105.49(3)	Se1-Cu1-I2	115.81(7)	Cu2-Cu4	2.752(1)
Se2-Cu-Br	109.23(2)	Se2-Cu1-I1#1	103.24(3)	Se2-Cu1-I2	112.76(6)	Cu3-Cu4	2.893(2)
Se1-Cu-Br#1	109.86(3)	Se1-Cu1-I1#1	110.27(3)	Se1-Cu1-Cu2	129.31(8)	I1-Cu1	2.646(8)
Se2-Cu-Br#1	102.03(2)	Se2-Cu1-I1#1	103.24(3)	Se2-Cu1-Cu2	129.04(7)	I1-Cu2	2.656(1)
Br-Cu-Br#1	111.21(2)	I1-Cu1-I1#1	115.71(2)	I2-Cu1-Cu2	61.88(4)	I1-Cu3	2.705(1)
Se1-Cu-Cu#1	126.87(3)	Se1-Cu1-Cu1#1	125.23(4)	Se1-Cu1-I1	100.35(6)	I2-Cu4	2.653(1)
Se2-Cu-Cu#1	118.37(3)	Se2-Cu1-Cu1#1	122.35(3)	Se2-Cu1-I1	105.43(6)	I2-Cu1	2.691(1)
Br-Cu-Cu#1	56.27(2)	I1-Cu1-Cu1#1	58.30(2)	I2-Cu1-I1	120.14(6)	I2-Cu2	2.777(9)
Br#1-Cu-Cu#1	54.94(2)	I1#1-Cu1-Cu1#1	57.41(2)	Cu2-Cu1-I1	58.29(4)	I3-Cu2	2.601(1)
				Se3-Cu2-Se4	99.34(6)	I3-Cu3	2.698(1)
				Se3-Cu2-I1	116.87(7)	I3-Cu4	2.770(9)
				Se4-Cu2-I1	115.09(7)	I4-Cu3	2.631(8)
				Se3-Cu2-Cu1	129.65(7)	I4-Cu4	2.680(1)
				Se4-Cu2-Cu1	128.16(7)	I4-Cu1	2.697(1)
				I1-Cu2-Cu1	61.36(4)	Se1-Cu1-I1	110.34(4)
				Se3-Cu2-I2	102.47(6)	Se1-Cu1-I2	102.11(3)
				Se4-Cu2-I2	100.35(6)	I1-Cu1-I2	111.83(3)

183

	I1-Cu2-I2	119.54(6)	Se1-Cu1-I4	110.88(4)
	Cu1-Cu2-I2	58.21(4)	I1-Cu1-I4	113.79(3)
			I2-Cu1-I4	107.24(3)
			Se2#1-Cu2-I3	114.01(4)
			Se2#1-Cu2-I1	109.93(4)
			I3-Cu2-I1	111.85(3)
			Se2#1-Cu2-I2	95.42(3)
			I3-Cu2-I2	115.59(3)
			I1-Cu2-I2	108.88(3)
			Se3-Cu3-I4	112.80(4)
			Se3-Cu3-I3	100.81(3)
			I4-Cu3-I3	111.04(3)
			Se3-Cu3-I1	109.89(3)
			I4-Cu3-I1	113.99(3)
			I3-Cu3-I1	107.39(3)
			Se4#2-Cu4-I2	112.31(4)
			Se4#2-Cu4-I4	109.24(4)
			I2-Cu4-I4	108.88(3)
			Se4#2-Cu4-I3	104.63(4)
			I2-Cu4-I3	114.12(3)
			I4-Cu4-I3	107.43(3)

184